AIP | Applied Physics Letters

Generation of equal-intensity coherent optical beams by binary geometrical phase on metasurface

Zheng-Han Wang, Shang-Chi Jiang, Xiang Xiong, Ru-Wen Peng, and Mu Wang

Citation: Applied Physics Letters **108**, 261107 (2016); doi: 10.1063/1.4955034
View online: http://dx.doi.org/10.1063/1.4955034
View Table of Contents: http://scitation.aip.org/content/aip/journal/apl/108/26?ver=pdfcov
Published by the AIP Publishing

Generation of equal-intensity coherent optical beams by binary geometrical phase on metasurface

Zheng-Han Wang, Shang-Chi Jiang, Xiang Xiong, Ru-Wen Peng,[a] and Mu Wang[a]
National Laboratory of Solid State Microstructures and School of Physics, and Collaborative Innovation Center of Advanced Microstructures, Nanjing University, Nanjing 210093, China

(Received 4 April 2016; accepted 18 June 2016; published online 30 June 2016)

We report here the design and realization of a broadband, equal-intensity optical beam splitter with a dispersion-free binary geometric phase on a metasurface with unit cell consisting of two mirror-symmetric elements. We demonstrate experimentally that two identical beams can be efficiently generated with incidence of any polarization. The efficiency of the device reaches 80% at 1120 nm and keeps larger than 70% in the range of 1000–1400 nm. We suggest that this approach for generating identical, coherent beams have wide applications in diffraction optics and in entangled photon light source for quantum communication. *Published by AIP Publishing.*
[http://dx.doi.org/10.1063/1.4955034]

A beam splitter changes an incident beam into two or more beams, and is an important optical component for quantum communication,[1–5] quantum computation,[6–9] optical interferometry,[9–12] etc. Traditionally, there are a number of ways to construct a beam splitter. It can be made of a cube by two glass prisms glued together with transparent resin. An incident light beam can be partially reflected and partially transmitted at the glass–resin interface. The thickness of the resin layer is often used to adjust the power splitting ratio for a certain wavelength range. Besides, by using dielectric coating with different thicknesses, a dielectric mirror can be applied as a beam splitter with wide range of power splitting ratio. In addition, a layer of thin metal film can also realize simultaneous transmission and reflection with different power splitting ratio. In modern optics, beams with exactly identical intensity and exactly the same polarization status are often required in order to investigate some fundamental quantum phenomena, such as quantum superposition and quantum randomness.[1–12] However, practically, equal-intensity beam splitting is not easy to realize. In particular, with traditional approach even though sometime equal-intensity beam splitting can be managed at a certain wavelength, a broadband functionality remains challenging.

The emergence of metasurface offers a unique approach to control the status of propagation of light beam.[13–27] Electromagnetic metasurface consists of arrays of specially designed sub-wavelength building blocks on a surface, which interacts with light so strongly that the amplitude, phase, polarization, and propagation direction of light can be effectively tuned. On a metasurface, the phase gradient is generated mainly based on geometrical symmetry of the building block.[18–27] Indeed by assembling rotating metallic split-rings[20,21] or single bars,[18,19,22,26] a geometry-induced phase gradient (sometime referred as Pancharatnam–Berry phase) is established, and circularly polarized beams with different handedness and different propagation directions are generated.[20,22]

In this letter we report a broadband optical beam-splitter based on the dispersion-free binary geometrical phase on a metasurface structure. The incident light with any polarization state can be split into two beams with exactly identical amplitude, phase, and polarization state yet with different propagation directions. This broadband optical beam splitter exhibits high energy utilization efficiency. The maximum efficiency of this device reaches 80% at 1120 nm and keeps larger than 70% in the range of 1000–1400 nm.

The building block of the equal-intensity optical beam splitter is made of a pair of parallel silver bars. The double-bars (DBS) pointing to 135° and 45° are denoted as DBS1 and DBS2, respectively. The silver structures sit on the SiO_2-silver-bilayer-capped silicon substrate. Before investigating the properties of combination of DBS1 and DBS2, the optical feature of a metasurface made of DBS1 only is studied. Figure 1(a) illustrates the details of DBS1. The optical properties of DBS1 are calculated based on finite difference time domain (FDTD) method. The parameters related to silver are obtained from the Drude model $\varepsilon(\omega) = 1 - \omega_p^2/(\omega^2 + i\omega_\tau\omega)$, where ω_p is the plasma frequency and ω_τ is the damping constant. For silver, we take $\omega_p = 1.37 \times 10^{16}$ rad/s and $\omega_\tau = 2.73 \times 10^{13}\,s^{-1}$.[28,29] The refractive index of the SiO_2 layer is taken as 1.45. The coordination is so set that the incident light propagates in –*z*-direction and the polarization is in *y*-direction. Due to the bottom silver reflection layer, the incident light cannot penetrate the substrate. R_{yy} and R_{xy} are defined as the intensity of *y*- and *x*-polarized reflected light with *y*–polarized normal incidence. When a linearly polarized incidence is reflected on an anisotropic structure, the polarization of the reflected light can be partly changed from its original direction to the orthogonal direction, which is known as the polarization conversion effect.[23,27,30,31] In our system, the incident light is linearly polarized in *x*- or *y*-direction, and the polarization can be decomposed into two perpendicular components, along the long and the short axis of the resonator, respectively. The silver bars interact with the incident electric field, and the reflection amplitudes in the two perpendicular components are identical while the relative phase retardation is 180°. In this situation, the linear polarization conversion occurs when the incidence

[a]Authors to whom correspondence should be addressed. Electronic addresses: rwpeng@nju.edu.cn and muwang@nju.edu.cn.

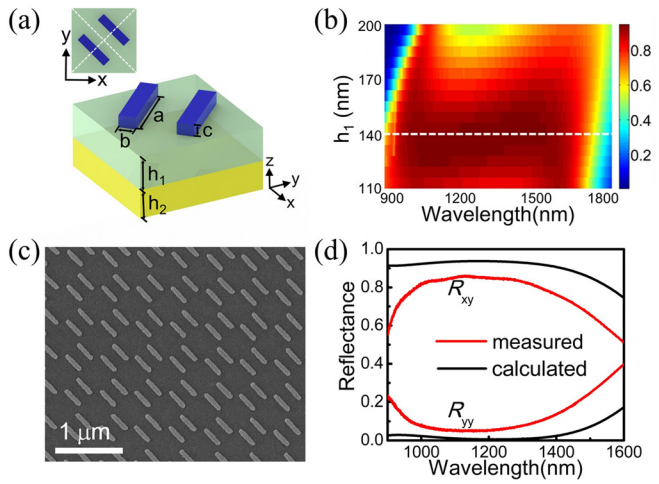

FIG. 1. (a) The building block of the metasurface. The detail topography of the designed building block is: the length a, width b, and height c of the silver bar are 300 nm, 70 nm, 50 nm, respectively. The thickness of the SiO_2 layer h_1 and silver layer h_2 are 140 nm and 120 nm, respectively. The lattice parameter is 500 nm. (b) The polarization conversion ratio of the structure is calculated as a function of interlayer thickness. The color represents the polarization conversion ratio. As marked by the white dash line, the maximum bandwidth and the largest polarization conversion ratio are realized when the thickness of the SiO_2 layer is 140 nm. (c) The SEM micrograph of DBS1. (d) The calculated and measured normal reflectance of the building blocks.

polarization is along either ***x***- or ***y***-axis.[23,27] We define the polarization conversion ratio (PCR) as the ratio of intensities of the cross-polarized reflected light and that of the incident light. The PCR as a function of wavelength and the thickness of SiO_2 interlayer (h_1) is plotted in Fig. 1(b). One may find that by selecting the interlayer thickness as 140 nm, the PCR can reach over 90% within a broad wavelength range (1000–1400 nm) for normal incidence.

A metasurface made of DBS1 only has been fabricated by electron beam lithography (EBL) on a SiO_2-silver-bilayer-capped silicon substrate, where the thickness of SiO_2 layer is 140 nm and that of the silver layer is 120 nm. The normal reflection spectrum is measured by a Fourier transform infrared spectrometer (FTIR) (Bruker vertex v70) combined with an infrared microscope (Hyperion 3000). A Fourier transform infrared spectrometer (Bruker vertex v70) combined with an infrared microscope (Hyperion 3000) is applied to measure the normal reflection. The microscope is equipped with a liquid-nitrogen-cooled MCT detector (D-316/B) (1000 nm–16 000 nm). Figure 1(d) indicates that over 70% PCR is realized in the range of 1000–1400 nm, and the maximum PCR of 80% is achieved at 1120 nm. This indicates that with DBS1 most energy of ***y***-polarized incidence has been converted to ***x***-polarized reflection. Comparing with simulation, the measured PCR is smaller, which could be due to the imperfection in sample fabrication.

Similarly, the feature of broadband optical polarization conversion can be realized with DBS2 as well. Due to the mirror symmetry of DBS1 and DBS2, there is a 180° phase difference between ***x***-polarization of light reflected by DBS1 and that by DBS2 for the same ***y***-polarized incidence. Therefore, once DBS1 and DBS2 are combined on the same surface, due to the superposition of electric fields, ***x***-polarized normal reflection will theoretically vanish. In practical application, no reflection along the axis of incidence beam is a preferred scenario.

Based on this idea, we design a metasurface with both DBS1 and DBS2, as shown in Fig. 2(a). The unit cell is made of two subsets, A and B. Subset A consists of three DBS1 while subset B consists of three DBS2. The lattice parameter of each building block is 500 nm, so the unit cell size in ***x***-direction of the metasurface is 3000 nm. Suppose the incident light propagates in $-z$ and is ***y***-polarized. We can first calculate the superposition of the ***y***-polarized reflection light. Since the width of building block is smaller than the wavelength, the ***y***-polarized light reflected by the building blocks can be treated as a plane wave propagating along $+z$ direction. Since both DBS1 and DBS2 have a large PCR, for ***y***-polarized normal incidence, ***y***-polarized reflection light is essentially zero.

Now we focus on the superposition of ***x***-polarized reflections. The 180° phase difference between the ***x***-polarized light reflected by DBS1 and DBS2 exists, and the phase distribution along ***x***-direction of the metasurface forms a binary function as shown in Fig. 2(b). Due to the periodic structures on the surface, the reflection follows:

$$\sin\theta_m = \frac{m}{D}\lambda, \tag{1}$$

where θ_m is the reflection angle, λ is the wavelength, D is the unit cell size in x-direction (3000 nm in our case), and m is an integer. In Eq. (1), to fulfill the requirement $|\sin\theta_m| \le 1$, and since wavelength λ is limited in the range of 1000–1400 nm, m should be taken as 0, ±1, ±2. Since the geometry offset between A and B is $D/2$, the difference of optical path between the light reflected by the two subsets in θ_m direction is $\frac{D}{2}\sin\theta_m$. The total optical path difference is $\frac{D}{2}\sin\theta_m + \frac{\lambda}{2}$, where the $\frac{\lambda}{2}$ term is introduced by the binary phase distribution along ***x***-direction. From Eq. (1) we get the difference of the optical path between A and B within a unit cell as $\frac{(m+1)\lambda}{2}$. When m is even, the diffraction from A and B possesses a phase difference of π and hence vanishes. For normal reflection ($m = 0$), as we indicated earlier, a phase difference of π exists, so there will be no normal reflection. It follows that the allowed value of m can only be ±1. Consequently, for ***y***-polarized normal incidence, the reflection by the metasurface contains two identical beams ($m = \pm1$), as shown in Fig. 2(c), where $\vec{k}_{+1}$ and $\vec{k}_{-1}$ represent the wave vectors of the ***x***-polarized diffraction with m equals to $+1$ and -1 in x-z plane, respectively. In this way an equal-intensity beam splitter is realized for normal incidence.

The propagation direction θ is calculated from Eq. (1) as a function of wavelength, as shown in Fig. 2(d). Figure 2(e) shows the FDTD-simulated ***x***-component of electric field distribution at 1000 nm. The wave fronts for diffraction $m = \pm1$ propagate in $\theta = \pm27.82°$, which is in good agreement with Eq. (1).

Due to the symmetry of DBS1 and DBS2, when the incidence is ***x***-polarized, the phase difference of ***y***-polarized reflection from DBS1 and DBS2 also possesses a phase difference of π. The phase distribution along ***x***-direction of the metasurface also possesses a binary distribution. Meanwhile

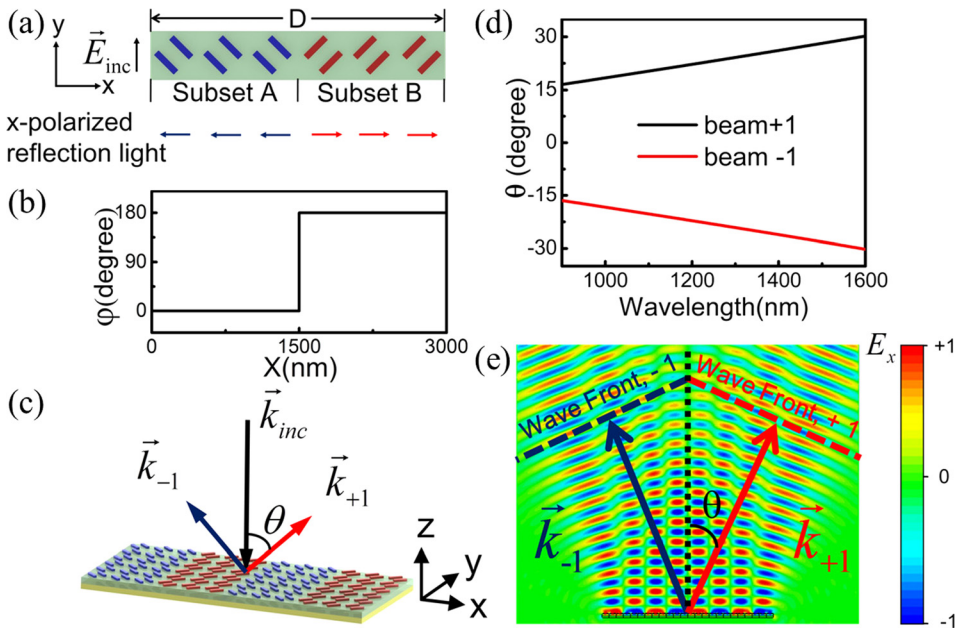

FIG. 2. (a) The micrograph of the unit cell of the metasurface, which consists of symmetric subsets, A and B. The normal incidence is ***y***-polarized. The polarization of the reflected light is converted to ***x***-polarization because of the building blocks. Due to the mirror symmetry of subsets A and B, the polarization of the reflected light has two directions, blue and red (left and right), respectively. (b) The phase difference of the ***x***-polarized reflection light along the ***x***-direction of the surface. (c)The schematic shows the direction of the incident light and reflected light. $\vec{k}_{inc}$ represents the ***y***-polarized normal incidence and $\vec{k}_{+1}$ and $\vec{k}_{-1}$ represent the wave vector of the ***x***-polarized diffraction light with m equal to +1 and −1, respectively. (d) The propagation angle of the diffraction beams calculated based on Eq. (1). (e) The simulated electric field distribution of ***x***-component with a 1400 nm ***y***-polarized normal incident beam.

the output is two identical ***y***-polarized diffraction beams with m = +1 and m = −1, respectively. The intensity of the two beams is identical since PCR for ***y***- and ***x***-polarized incidence is identical. In this way two identical beams can be generated with an incidence of any polarization. We need to point out that our beam-splitter is designed for normal incidence. Unless the deviation from normal incidence is small, otherwise PCR of our symmetric building block drops, and broadband feature disappears gradually as the deviation increases.

To verify the calculated results, we fabricate a metasurface made of subsets A and B with electron beam lithography (Fig. 3(a)), where the total size of the sample reaches 1 mm × 1 mm. A Fourier transform infrared spectrometer (Bruker vertex v70) combined with an infrared microscope is applied to measure the normal reflection. For the oblique diffraction measurement, an angle-resolved vis-IR spectroscopy system (Fig. 3(b)) is applied, where a super-continuum laser combined with a monochromator generates the monochromatic light. A polarizer is applied in the incident beam to regulate its polarization, and a CaF_2 lens (f = 80 mm) focuses the incident light onto the sample. To characterize the spectrum of the oblique diffraction light, another CaF_2 lens (f = 80 mm), a polarizer, and a germanium photodiode detector are placed on a motorized rotation stage. Spectrum is measured by sweeping the rotation angle θ from −40° to 40°.

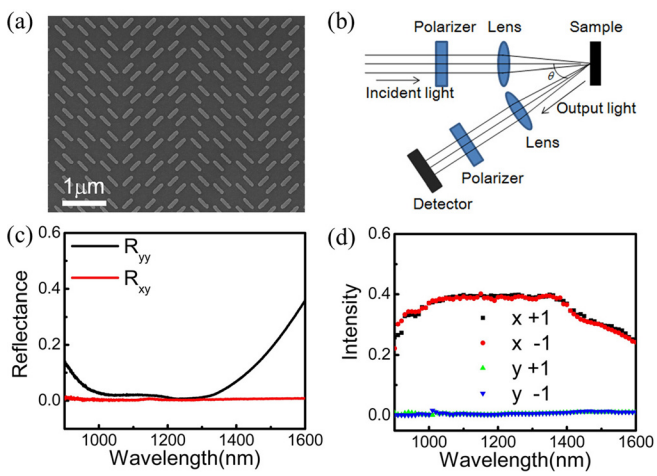

FIG. 3. (a) The SEM micrograph of the experimentally fabricated metasurface. (b) The schematic diagram of the angle-resolved setup to measure the intensity of diffraction beam. (c) The measured normal reflectance of ***x***- and ***y***-polarizations of the normal reflection beam. (d) The measured intensity of ***x***-and ***y***-polarization of the diffraction beams +1,−1.

As illustrated in Fig. 3(c), for a ***y***-polarized incidence propagating in −***z***-direction, both ***x***- and ***y***-polarized normal reflection (along +***z***-direction) is smaller than 5% when the wavelength is in the range of 1000–1400 nm.

For ***y***-polarized normal incident light, the oblique reflection from the metasurface contains two identical beams with ***x***-polarization, indicating that with monochromatic incidence, energy can only be detected in the direction θ_m with m = +1 and m = −1. With the angle-resolved vis-IR spectroscope described above (Fig. 3(b)) we measure the spectra, as shown in Fig. 3(d). Two diffraction beams m = +1 and m = −1 are polarized within *x*-*z* plane, and their intensity are identical. The total intensity of these beams reaches 80% of the incidence at 1120 nm. The intensity of the diffracted beams at the other frequencies (wavelength 1000–1400 nm) is higher than 70% of the incident light in average. These data show that the metasurface indeed functions as a beam splitter with identical intensity and polarization state in a broad frequency range with high efficiency.

Excited by incident electromagnetic waves, free electrons on the metal surface oscillate and affect the surrounding electromagnetic field by radiation. At the resonant frequency, this effect is so significant that a thin layer of metallic structure can effectively tune the state of light. However, the Lorentz resonance in metal is highly dispersive in nature, which limits its application to a narrow wave band. On the other hand, dielectric material interacts with light by accumulating an optical path within a certain thickness. This feature is effective over a broad bandwidth and has already been applied in antireflection coating and other optical

devices. By integrating a metallic metastructure with a dielectric interlayer, the intrinsic dispersion of the metallic structures can be cancelled out by the thickness-dependent dispersion of the dielectric spacing layer.[31] In this way, the large polarization conversion effect of our metastructure can be realized over a broad wavelength range. The double-bar metasurface structures provide better broadband feature than the single-bar metasurface.

To summarize, we demonstrate here the generation of equal-intensity coherent optical beams by binary geometrical phase on a metasurface. By introducing mirror-symmetric building blocks, a binary phase metasurface is realized. Since the binary phase does not rely on the optical property of building blocks, such a beam splitter is dispersion-free. The building block with large polarization conversion ratio enables the high efficiency of the binary phase metasurface. We have demonstrated that the efficiency of this device may reach 80% at 1120 nm and keeps higher than 70% in average in the range of 1000–1400 nm. Since equal-intensity beam splitter can be widely used in generating entangled two photon light source for the quantum communication and in exploring some fundamental quantum phenomena, it is highly desired to develop equal-intensity coherent optical beam splitters with dispersion-free feature. Our current study provides a unique design to fulfill these requirements.

The authors acknowledge the grants from the State Key Program for Basic Research from MOST of China (Grant Nos. 2010CB630705 and 2012CB921502) and from NSF of China (Grant Nos. 11474157, 11574141 and 61475070).

[1]K. Mattle, H. Weinfurter, P. G. Kwiat, and A. Zeilinger, Phys. Rev. Lett. **76**, 4656 (1996).
[2]D. Bouwmeester, J.-W. Pan, M. Daniell, H. Weinfurter, and A. Zeilinger, Phys. Rev. Lett. **82**, 1345 (1999).
[3]J. Brendel, N. Gisin, W. Tittel, and H. Zbinden, Phys. Rev. Lett. **82**, 2594 (1999).
[4]L.-M. Duan, M. Lukin, J. I. Cirac, and P. Zoller, Nature **414**, 413 (2001).
[5]R. Ursin, F. Tiefenbacher, T. Schmitt-Manderbach, H. Weier, T. Scheidl, M. Lindenthal, B. Blauensteiner, T. Jennewein, J. Perdigues, and P. Trojek, Nat. Phys. **3**, 481 (2007).
[6]D. Bouwmeester, J.-W. Pan, K. Mattle, M. Eibl, H. Weinfurter, and A. Zeilinger, Nature **390**, 575 (1997).
[7]E. Knill, R. Laflamme, and G. J. Milburn, Nature **409**, 46 (2001).
[8]A. Furusawa, J. L. Sørensen, S. L. Braunstein, C. A. Fuchs, H. J. Kimble, and E. S. Polzik, Science **282**, 706 (1998).
[9]D. E. Browne and T. Rudolph, Phys. Rev. Lett. **95**, 010501 (2005).
[10]P. Grangier, G. Roger, and A. Aspect, Europhys. Lett. **1**, 173 (1986).
[11]F. Riehle, T. Kisters, A. Witte, J. Helmcke, and C. J. Bordé, Phys. Rev. Lett. **67**, 177 (1991).
[12]J. L. O'Brien, G. J. Pryde, A. G. White, T. C. Ralph, and D. Branning, Nature **426**, 264 (2003).
[13]N. Yu, P. Genevet, M. A. Kats, F. Aieta, J. P. Tetienne, F. Capasso, and Z. Gaburro, Science **334**, 333 (2011).
[14]S. Sun, K. Y. Yang, C. M. Wang, T. K. Juan, W. T. Chen, C. Y. Liao, Q. He, S. Xiao, W. T. Kung, G. Y. Guo, L. Zhou, and D. P. Tsai, Nano Lett. **12**, 6223 (2012).
[15]N. Yu, F. Aieta, P. Genevet, M. A. Kats, Z. Gaburro, and F. Capasso, Nano Lett. **12**, 6328 (2012).
[16]F. Aieta, M. A. Kats, P. Genevet, and F. Capasso, Science **347**, 1342 (2015).
[17]M. Kang, T. Feng, H.-T. Wang, and J. Li, Opt. Express **20**, 15882 (2012).
[18]L. Huang, X. Chen, H. Muhlenbernd, G. Li, B. Bai, Q. Tan, G. Jin, T. Zentgraf, and S. Zhang, Nano Lett. **12**, 5750 (2012).
[19]L. Huang, X. Chen, B. Bai, Q. Tan, G. Jin, T. Zentgraf, and S. Zhang, Light: Sci. Appl. **2**, e70 (2013).
[20]S.-C. Jiang, X. Xiong, Y.-S. Hu, S.-W. Jiang, Y.-H. Hu, D.-H. Xu, R.-W. Peng, and M. Wang, Phys. Rev. B **91**, 125421 (2015).
[21]L. Liu, X. Zhang, M. Kenney, X. Su, N. Xu, C. Ouyang, Y. Shi, J. Han, W. Zhang, and S. Zhang, Adv. Mater. **26**, 5031 (2014).
[22]D. Wen, F. Yue, G. Li, G. Zheng, K. Chan, S. Chen, M. Chen, K. F. Li, P. W. H. Wong, and K. W. Cheah, Nat. Commun. **6**, 8241 (2015).
[23]Y. Xu, Y. Fu, and H. Chen, Sci. Rep. **5**, 12219 (2015).
[24]F. Ding, Z. Wang, S. He, V. M. Shalaev, and A. V. Kildishev, ACS Nano **9**, 4111 (2015).
[25]A. V. Kildishev, A. Boltasseva, and V. M. Shalaev, Science **339**, 1232009 (2013).
[26]G. Zheng, H. Mühlenbernd, M. Kenney, G. Li, T. Zentgraf, and S. Zhang, Nat. Nanotechnol. **10**, 308 (2015).
[27]Y. Yang, W. Wang, P. Moitra, I. I. Kravchenko, D. P. Briggs, and J. Valentine, Nano Lett. **14**, 1394 (2014).
[28]P. B. Johnson and R.-W. Christy, Phys. Rev. B **6**, 4370 (1972).
[29]M. A. Ordal, R. J. Bell, R. W. Alexander, L. L. Long, and M. R. Querry, Appl. Opt. **24**, 4493 (1985).
[30]Q. Lévesque, M. Makhsiyan, P. Bouchon, F. Pardo, J. Jaeck, N. Bardou, C. Dupuis, R. Haïdar, and J.-L. Pelouard, Appl. Phys. Lett. **104**, 111105 (2014).
[31]S.-C. Jiang, X. Xiong, Y.-S. Hu, Y.-H. Hu, G.-B. Ma, R.-W. Peng, C. Sun, and M. Wang, Phys. Rev. X **4**, 021026 (2014).